Phase Behavior of Poly(4-vinylpyridine)/Poly(vinyl acetate-*co*-vinyl alcohol) Blends

Luis C. Cesteros, José R. Isasi, and Issa Katime*

Grupo de Nuevos Materiales, Departamento de Química Física, Facultad de Ciencias, Campus de Leioa, Universidad del País Vasco, Apartado 644, Bilbao, Spain

Received December 28, 1993; Revised Manuscript Received September 21, 1994®

ABSTRACT: The phase behavior of poly(4-vinylpridine) (P4VP)/poly(vinyl acetate-*co*-vinyl alcohol) (ACA) blends has been studied as a function of ACA copolymer composition. Calorimetric curves for blends of ACA ranging from 23 to 53% of vinyl alcohol units show exothermal peaks above the glass transition corresponding to phase separation processes. Heats of the mixing of about 1.5 cal/g have been obtained. A progressive breaking of H-bonds as temperature increases is detected by IR spectroscopy. Cloud point curves obtained by optical microscopy measurements depend on ACA copolymer composition. The binary interaction model has been applied to this system from cloud point data.

Introduction

In previous papers we have studied the miscibility and specific interactions in poly(4-vinylpyridine) (P4VP)/poly(vinyl acetate-*co*-vinyl alcohol) (ACA) blends using DSC and FTIR.[1,2] Their phase diagrams at room temperature show a miscibility window for the intermediate region of ACA copolymer compositions. The upper limit (high contents in vinyl alcohol units) seems to depend on the high level of self-association for pure poly(vinyl alcohol), while the lower one is related to the low number of favorable hydroxyl–pyridine interactions for minor hydroxyl contents in these ACA copolymers. In the latter situation, thermal analysis permits to detect phase separation for blends with ACA copolymers ranging from 20 to 50% degree of hydrolysis. For these blends, close to phase separation limits, the temperature plays an important role on miscibility: specific interactions, which are of a highly directionally dependent nature, are present in these blends. As temperature increases, the number of directional specific interactions is reduced by the thermal motion. Besides, the balance between the different types of hydrogen bonds that are present in the mixture (hydroxyl–hydroxyl, hydroxyl–carbonyl, and hydroxyl–pyridine) depends on temperature because of their characteristic enthalpies of H-bond formation and equilibrium constants.

In this paper phase separation processes for these blends are studied in detail. DSC and optical microscopy were used to investigate phase separation. FTIR was also employed to study the temperature behavior of the specific interactions involved in these systems.

Experimental Section

Materials. Poly(4-vinyl pyridine) (P4VP) was a commercial sample kindly supplied by Reilly Chemicals (sample 450). Its weight-average molar mass determined by light scattering was 49 000 g/mol. The sample was purified by precipitation from methanol into ether.

Poly(vinyl acetate) (PVAc) (Erquimia S.A.; sample B-1000) was purified by dissolution in acetone and precipitation into ether petroleum followed by dissolution in methanol and reprecipitation in water. PVAc was characterized by GPC in THF. Molar mass and index of polydispersity were calculated according to the univeral calibration procedure taking as viscometric equation for PVAc in THF: $[\eta] = 0.035\ M^{0.63}$ The results were 255 000 g/mol and 2.1 for molar mass and index of polydispersity, respectively. ACA copolymers employed in this study have been prepared from poly(vinyl acetate) according to standard procedures previously described.[1] Copolymer compositions and sequence distributions have been determined by NMR spectroscopy using a Bruker AC-250 spectrometer.[3] The ACA copolymers employed in this work have quasi-random comonomer sequence distributions. Their degree of hydrolysis is 23.3 (ACA23), 34.1 (ACA34), 39.4 (ACA39), and 53.3% (ACA53).

Calorimetric Measurements. Thermal analysis was performed on a Mettler TA 4000 system equipped with a DSC30 measuring cell. A heating rate of 20 K/min was used if not specified otherwise. Sample sizes ranged from 10 to 15 mg.

Cloud point curves in ACA/P4VP blends were investigated by means of thermooptical analysis. The films were cast onto glass microscope slides from 2% (w/v) methanol solutions and placed in a Mettler FP82 hot stage device. The system was placed under a Jenapol microscope (Carl Zeiss, Jena, ltd.) equipped with a photoelectric cell. All the scans start from 403 K, after 3 min of annealing at this temperature in order to avoid moisture and solvent residues. The cloud points were detected as the onset of the transmitted light jump.

Infrared Measurements. The infrared spectra for the blends were recorded on a Nicolet-520 fourier transform infrared spectrometer with a resolution of 2 cm^{-1}, and 100 scans were averaged. Films for FTIR measurements were cast from methanol solutions (0.02 g/mL) directly on KBr pellets. All films were vacuum-dried, and they were thin enough to be within the absorbance range where the Beer–Lambert law is obeyed. The influence of temperature on the spectral features of the blends was studied by using a Specac variable temperature cell, P/N 21.5000. Temperature was controlled with a Eurotherm 847 unit.

Results and Discussion

Heat of Demixing. As we have reported in a previous study,[1] calorimetric results show phase separation processes for blends P4VP/ACA where the ACA copolymer has a degree of hydrolysis above the lower miscibility limit (20%). For instance, a blend of a 29% hydrolyzed ACA with 60 wt % of P4VP subjected to successive scans, each one to a higher end temperature, exhibits the gradual appearance of two distinct T_g's corresponding to the onset of two different phases. This LCST behavior was observed in the miscible blends where the copolymer has a degree of hydrolysis below 50%. For higher degree of hydrolysis, no phase separation is observed for annealing temperatures up to 500

* Address for correspondence: Dr. Issa Katime, Avenida Basagoiti, 8-1°C, Algorta, Vizcaya, Spain.

® Abstract published in *Advance ACS Abstracts,* November 1, 1994.

0024-9297/94/2227-7887$04.50/0

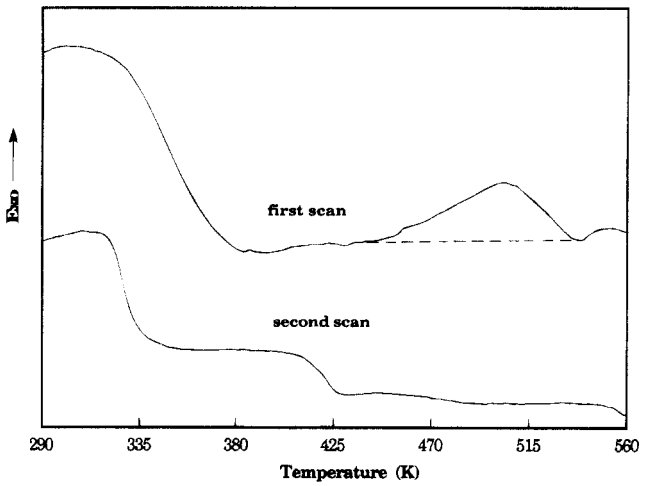

Figure 1. Consecutive DSC scans for the ACA34/P4VP blend (60:40, w/w).

Table 1. Heats of Demixing and Peak Positions at Different Heating Rates for the ACA34/P4VP (50:50, w/w) Blend

heating rate (K/min)	peak position (K)	heat of demixing (cal/g)
5	472	0.67
10	486	0.74
20	491	0.69
30	493	0.79
40	503	1.03
60	511	1.32

K (at higher temperatures ACA copolymers present thermal degradation processes).

Heats of demixing associated to LCST behavior can be detected by DSC.[4-8] Positive and negative values have been reported for different blends. Figure 1 shows the thermograms obtained for an ACA34 blend with 40 wt % of P4VP. The first scan, at a heating rate of 40 K/min, shows a single glass transition followed by an exothermal peak centered at 503 K. After a quick cooling, the consecutive scan shows two glass transitions close to those of the pure components of the blend. The phase separation observed is irreversible: phase redissolution does not seem to occur for these blends. The positions of the exothermal peaks (expressed as the location of the maximum) and areas depend on the heating rate, and they are displayed in Table 1 for a ACA34/P4VP (50:50, w/w) blend. An increase in the values of peak temperatures and areas is observed as heating rate increases. This is a common behavior for phase demixing processes in polymer blends.

The extrapolation of the demixing peak onset temperatures to zero heating rate (thermodynamic equilibrium condition) should give the corresponding pseudobinodal or "cloud point" in the phase diagram. Nevertheless, this is a quite imprecise method to obtain LCST curves due to the poor definition of the peaks as heating rate decreases. On the other hand, the extrapolation to large heating rates is related to the spinodal temperature,[7] but we have to consider that the spinodal decomposition is controlled by diffusion processes. At very high heating rates, the "plateau" value reached for the area of the exothermal peak can be considered as the demixing heat for the blend, providing that two pure component phases are obtained after the scan. This is the case for our blends since two T_g temperatures very close to those of pure components are obtained in the consecutive scans, as has been previously indicated (see Figure 1).

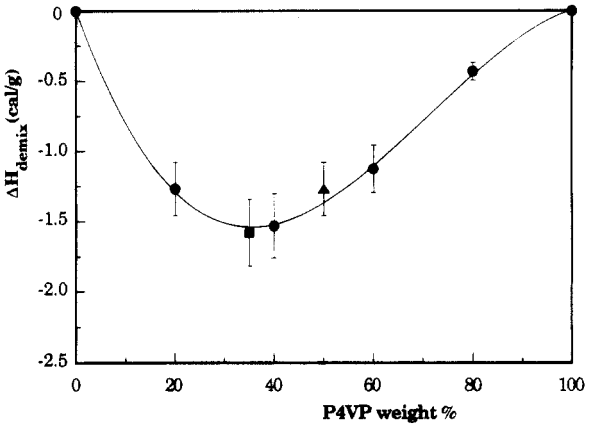

Figure 2. Heat of demixing for different ACA/P4VP blends: (■) ACA23, (●) ACA34, and (▲) ACA53.

For the system shown in Figure 1, the value obtained for the heat of demixing is 1.5 ± 0.1 cal/g (0.41 kcal/mol of P4VP). This value is in the order of that previously reported for other hydrogen-bonded blends[4,6,8] and lower than that reported for charge transfer interacting blends.[4] The value for the peak area gives an idea of the strength of the interactions between the components.

Figure 2 shows the heat of demixing for ACA34/P4VP blends as a function of blend composition. The values displayed have been obtained by averaging the results of two measurements at a high enough heating rate, 40 K/min. In the same plot, the results for two other blends of P4VP with other ACA copolymers (ACA23 and ACA53) are also displayed. According to these results, the heat of demixing does not exhibit a great dependence with copolymer composition in these systems. Nevertheless, the peak positions depend on the ACA copolymer employed (487 K for ACA23, 503 K for ACA34, and 548 K for ACA53, at 40 K/min) since they are related to LCST curve points (see below).

In the case of ACA53/P4VP blends, the last part of the exothermic peak overlaps with the onset of the thermal degradation but two T_g's are detected after this scan. On the contrary, no phase separation can be achieved by isothermal annealing of these blends, what can be considered as a consequence of the thermal degradation of the samples.

Phase Separation Evidences via FTIR Data. In previous works[2,9] dealing with hydrogen bonding in blends involving poly(vinylpyridines), we have shown that the pyridine ring mode at 993 cm^{-1} is the most appropriate band for the detection of hydrogen-bonded pyridine groups. Figure 3 shows several spectra for the same blend in this region. Digital subtraction of the contribution of the ACA component has been necessary because of the overlapping of the intense C−O stretching band of hydroxyl groups, although a qualitative discussion can be performed. The spectrum of the blend recorded at room temperature (after annealing at 403 K to avoid moisture and achieve thermal equilibrium above T_g) shows a significant contribution located at 1004 cm^{-1} corresponding to hydrogen-bonded pyridine groups. As temperature increases, this contribution becomes less significant, indicating the breaking of hydrogen bonds (see Figure 3). Nevertheless, the spectrum at 298 K of a cooled sample after scanning up to 473 K shows a recovery of hydrogen bonding, giving an idea of a reversible behavior. A sample heated up to 513 K, at 6 K/min, shows a different spectrum at

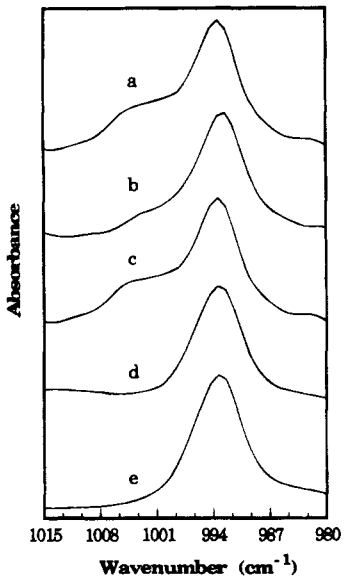

Figure 3. Scale-expanded infrared spectra in the range 980–1015 cm^{-1} for the ACA34/P4VP blend (50:50, w/w): (a) at 298 K after annealing at 400 K, (b) at 440 K, (c) at 298 K after annealing at 470 K, (d) at 298 K after annealing at 513 K, and (e) pure P4VP. The first four spectra have been digitally subtracted.

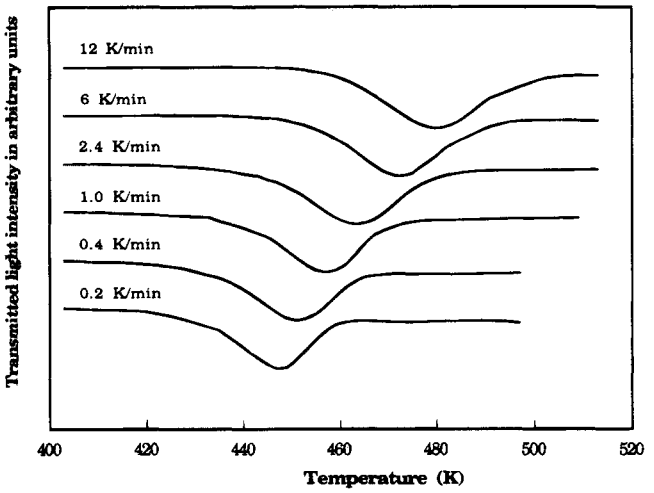

Figure 4. Transmitted light intensity as a function of temperature for thin films of ACA23/P4VP (65:35, w/w) at different heating rates.

room temperature after this thermal protocol: the contribution of associated pyridine groups has disappeared because of an irreversible rupture of hydrogen bonds. These results confirm that phase spearation takes place in this system.

Cloud Point Curves. Temperatures of phase separation in polymer blends can be obtained by various methods such as optical microscopy,[10] light scattering,[11] small angle X-ray scattering,[12] DSC measurements after annealing,[13] or DSC at high heating rates when a peak of demixing is observed.[5-8] Optical microscopy is an appropriate method when there is a fair difference in refractive index between the polymers involved in the blend. This is the case in our blends, since P4VP has a refractive index of 1.60, far enough from ACA copolymers (n = 1.46–1.50).

Figure 4 shows the results of the temperature–light transmission measurements for the blend ACA23/P4VP (65:35, w/w) at different heating rates from 0.2 to 12 K/min. For this sample the transmitted light intensity, I, starts to decrease over 413 K on heating and keeps on decreasing gradually until it reaches a minimum. After this point, the detected intensity increases, indicating that the film becomes transparent again; finally, a new "plateau" value is reached, whose level is close to the initial one. As can be seen in Figure 4, all these curves are similar (ca. 40–50 K wide) and a shift toward higher temperatures is observed with increasing the heating rate.

In order to obtain accurate results from this technique, two experimental conditions affecting film properties must be considered. Film thickness can affect cloud points since significant signal changes are achieved sooner with thicker films.[10] Besides, selective adsorptions on the substrate may also affect the results for extremely thin films.[14] In our case, the concentrations employed for the polymer solutions allow to obtain a sufficient thickness (ca. 50 μm) in order to avoid those mentioned effects. Since selective adsorption is possible and may result in different polymer concentrations on the glass slides,[14] the field of vision has been elected large enough compared to the total area of the film in order to minimize this possible effect.

In some systems the measured cloud points do not depend on the heating rate; for instance, in PMMA/PVAc blends, the cloud point curves measured at 2 and 20 K/min only differ by 1 or 2 K at most.[15] Nevertheless, this is not the general situation. The heating rate dependence is quite large in a poly(styrene)/poly(2-chlorostyrene) system.[16] The reason is that the cloud point is a kinetic rather than a thermodynamic property.[17,18] Besides, polymers are highly viscous materials with small diffusion coefficients, so extrapolation at isothermal condition (zero heating rate) is recommended.[10] The effect of heating rate, already shown in Figure 4, is clearly displayed in Figure 6 where extrapolations at zero heating rate for different blends with the same P4VP contents are plotted.

The photomicrographs in Figure 5 show the morphology of the ACA34/P4VP blend during the phase separation process for the sample heated at 6 K/min. At the first stages (corresponding to spinodal decomposition), the cloudiness of the sample increases gradually until the minimum of intensity. At 473 K an extremely dark pattern is detected. Then, at 483 K the sample becomes gray, and at 493 K small domains begin to separate. These domains grow as temperature increases, coarsening into droplets or interconnected structures. These structures merge as temperature increases, causing the clearing of the sample. In fact, these samples look quite clear to the naked eye after the thermal treatment because their phase-separated structures are large enough to allow light transmission. In contrast, samples quenched during earlier stages present a turbid aspect. The development of phase-separated structures after spinodal decomposition has already been studied in isothermal conditions for other blends,[11,19-22] and the mechanism of the coalescence process has also been explained.[23,24] In our systems the demixing process depends on heating rate, blend composition, and ACA copolymer composition. Dependence on heating rate can be clearly observed in Figure 6.

The blends containing ACA39 permit to detect a reversible behavior: on cooling these samples, they become clear, on heating them again, phase separation occurs newly, though it takes place at a lower temperature. This can be explained in terms of a partial phase recovery (by kinetic reasons) with a different composition for the mixed phase.

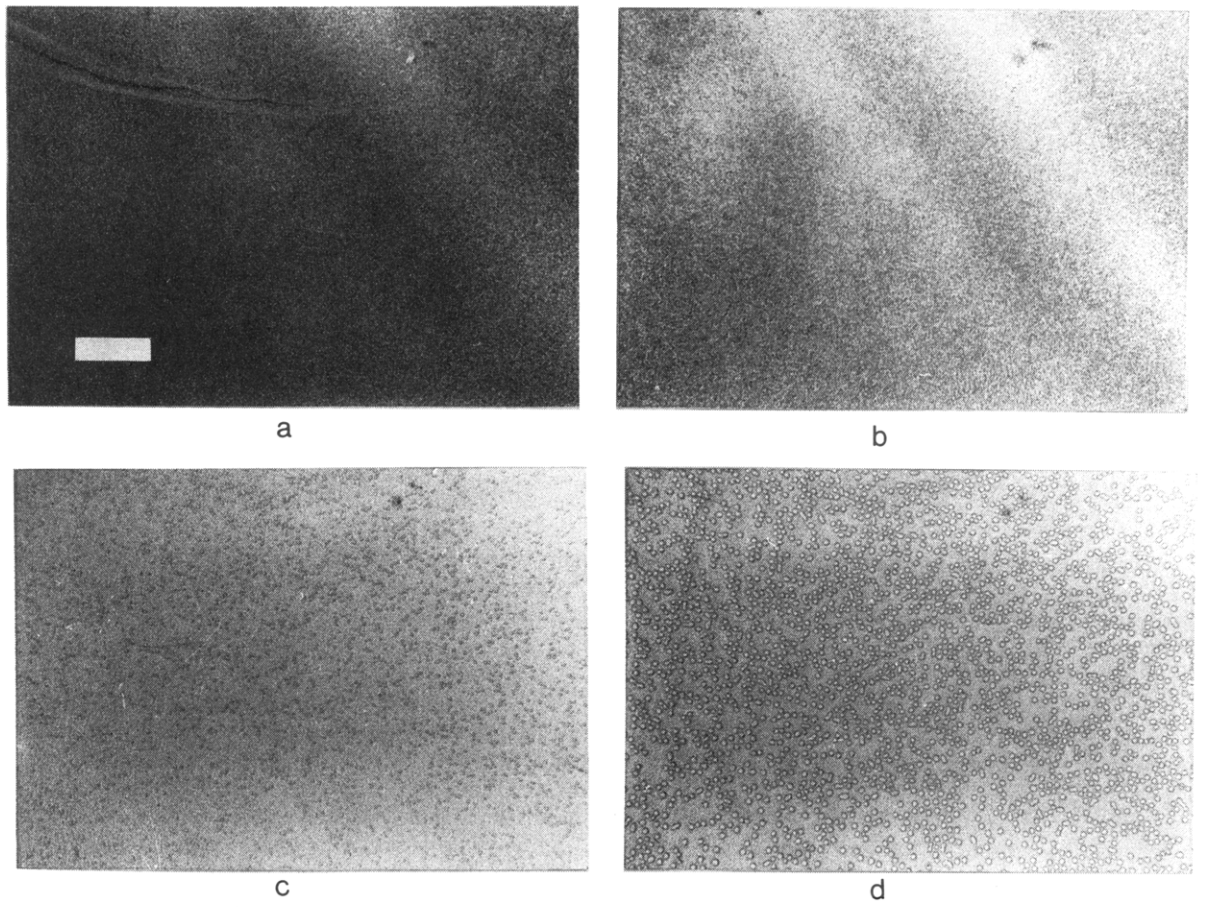

Figure 5. Optical micrographs of the ACA34/P4VP (50%) blend at different temperatures for a scan of 6 K/min: (a) 483 K, (b) 493 K, (c) 503 K, and (d) 513 K. White bar in the figure corresponds to 150 μm.

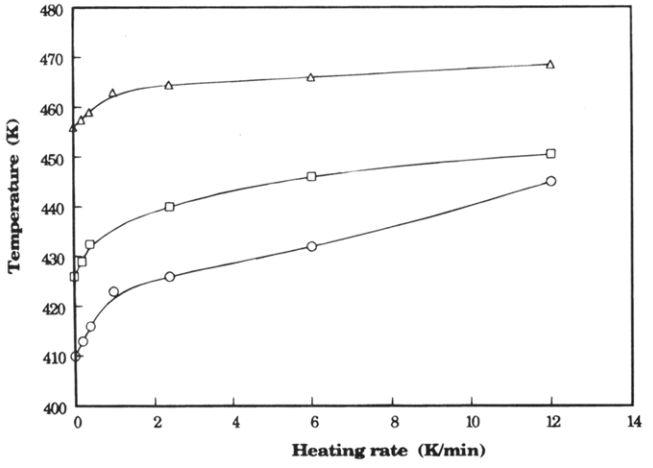

Figure 6. Dependence of cloud point temperatures on heating rate for different ACA/P4VP blends (65:35, w/w): (△) ACA 39, (□) ACA34, and (○) ACA23.

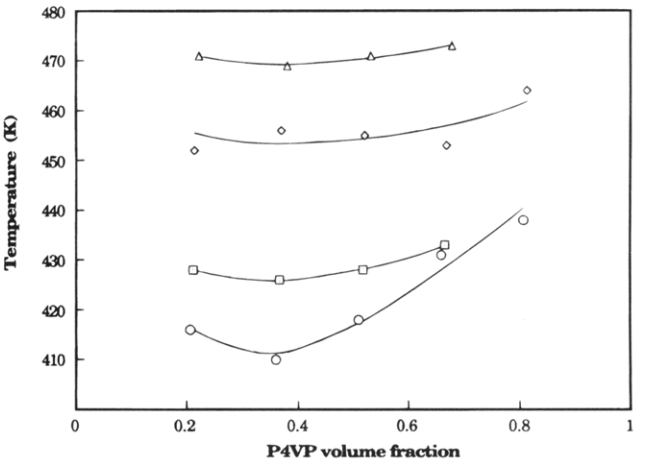

Figure 7. Cloud point curves for ACA/P4VP blends: (○) ACA23, (□) ACA34, (◇) ACA39, and (△) ACA53.

Figure 7 shows the cloud point curves for the blends studied in this work. They have been obtained by extrapolations of phase demixing temperatures at zero heating rate, as shown in Figure 6. Special care must be taken for ACA53/P4VP blend results, since the phase separation process is close to the thermal decomposition of ACA53. The extrapolations have been performed without considering the lowest heating rates since overlapping with the decomposition process is more probable in those cases.

As can be seen in Figure 7, the cloud point curves clearly depend on the ACA copolymer composition. As the content in hydroxyl units in the copolymer increases, the temperature of phase demixing for the blend increases, as expected. Besides, the blends with ACA copolymer of a high degree of hydrolysis exhibit cloud point curves almost independent of composition.

When the polydispersity of the polymer samples is not excessive (as in this work), the cloud point phase diagrams after extrapolation to zero heating rate will be sufficiently close to the coexistence or binodal curve.[25] The interaction parameter for the pairs of polymers studied in this work can be evaluated from the cloud point measurements.[25-27] These results have been fitted to the binodal curve calculated on the basis of the Flory Huggins equation (free energy of mixing per unit volume of the mixture):

$$\Delta G_M = RT[(\phi_1/V_1)\ln\phi_1 + (\phi_2/V_2)\ln\phi_2] + B\phi_1\phi_2 \quad (1)$$

where V_1 and V_2 are the molar volumes of polymers 1 and 2, ϕ_1 and ϕ_2 are the volume fractions of the two polymers, and B is the interaction energy density between the two.

The best fit to the experimental cloud points will be achieved by including the dependences of the B parameter on temperature and composition. Although for some blends the composition dependence has been found to be small,[26] we have included both dependences. The simplest functional form to incorporate them is[25,27]

$$B = b_0 + b_1\phi_1 + b_T T \quad (2)$$

The values of the constants b_0, b_1, and b_T giving the best fit have been determined by means of a nonlinear least squares fit method, and they are shown in Table 2.

Application of the Binary Interaction Model. The miscibility behavior of copolymer blends is often explained by using the binary interaction model.[28-30] This model gives the following expression for the overall blend interaction parameter of a homopolymer (A)/copolymer (BC) blend system:

$$B_{blend} = yB_{AB} + (1-y)B_{AC} - y(1-y)B_{BC} \quad (3)$$

where y is the volume fraction of B in the copolymer (vinyl alcohol units in our systems) and B_{ij} are the binary interaction energy densities. The criterion for miscibility is that $B_{blend} < B_{crit}$, where

$$B_{crit} = RT/2(V_1^{-1/2} + V_2^{-1/2})^2$$

The values of B_{blend} calculated from the data of Table 2 for different ACA/P4VP blends at 298 K and $\phi_1 = 0.5$ are displayed in Figure 8. Besides, we have earlier reported[1] the miscibility window obtained for this system with similar samples. This window is located between 21.5 and 97.0% of vinyl alcohol units, which are equivalent to volume fractions of 0.084 and 0.916 in the copolymer. These points correspond to critical values, i.e., $B_{blend} = B_{crit}$, and have also been plotted in Figure 8. The B_{ij} values for this system are easily calculated by fitting these points into eq 3. Their values are: 0.29, 0.25, and 3.24 cal/cm^3 for the A–B, A–C, and B–C pairs, respectively. Interestingly, a positive value (i.e., an indication of immiscibility of the corresponding polymer pair) is also obtained for B_{AB} if the experimental phase boundary at $y = 0.916$ is excluded in the fitting procedure. This event could be regarded as an adequate prediction of immiscibility for the PVA/P4VP pair by means of the binary interaction model.

The obtained results for B_{BC} and B_{AC} seem to be contrary to intuition, since a lower "repulsion" would be expected for the alcohol–acetate (B–C) pair compared to the acetate–pyridine (A–C) one. In fact hydrogen bonding between R and C units is detected by IR. The binary interaction model is specially adequate for systems without specific interactions, in which repulsion effects are predominant. Nevertheless, it can be applied to our system if we make several special considerations: although the B_{BC} parameter results are positive, this is not an indication of real repulsion, but it gives an idea on immiscibility for the corresponding homopolymer pair. In this way, immiscibility between those homopolymers can be explained considering that self-association of B units is favored vs interassociation with acetate groups. Then, the binary parameters would not be an indication of real repulsions but competing interactions.

Table 2. Polymer–Polymer Interaction Parameters[a] and Eq 2 Coefficients Determined from Cloud Point Measurements

copolymer	b_0 (cal cm^{-3})	b_1 (cal cm^{-3})	b_T (cal cm^{-3} K^{-1})	B (cal cm^{-3})
ACA23	−0.314	0.0813	0.00081	−0.0316
ACA34	−0.672	0.0810	0.00163	−0.1450
ACA39	−0.882	0.0736	0.00202	−0.2434
ACA53	−1.194	0.0792	0.00261	−0.3749

[a] At 298 K and $\phi_1 = 0.5$.

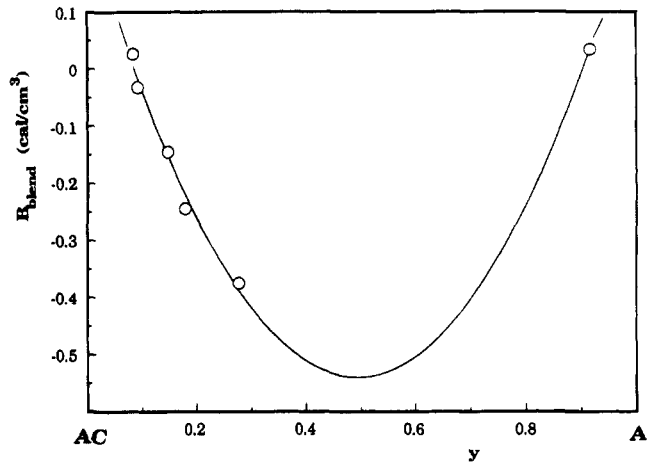

Figure 8. Values of B_{blend} for different ACA/P4VP blends at 298 K and $\phi_1 = 0.5$. The curve shows the fitting to eq 3.

Acknowledgment. The authors thank the CICYT (Project MAT 464/92-C02), CYTED, and Vicerrectorado de Investigación de la Universidad del País Vasco (UPV-92) for financial support. J.R.I. thanks the Departamento de Educación, Universidades e Investigación del Gobierno Vasco for a grant.

References and Notes

(1) Cesteros, L. C.; Isasi, J. R.; Katime, I. *J. Polym. Sci., Polym. Phys. Ed.* **1994**, *32*, 223.
(2) Cesteros, L. C.; Isasi, J. R.; Katime, I. *Macromolecules* **1993**, *26*, 7256.
(3) Isasi, J. R.; Cesteros, L. C.; Katime, I. *Macromolecules* **1994**, *27*, 2200.
(4) Natansohn, A. *J. Polym. Sci., Polym. Lett. Ed.* **1985**, *23*, 305.
(5) Ebert, M.; Garbella, R. W.; Wendorff, J. H. *Makromol. Chem., Rapid Commun.* **1986**, *7*, 65.
(6) Uriarte, C.; Eguiazábal, J. I.; Llanos, M.; Iribarren, J. I.; Iruin, J. J. *Macromolecules* **1987**, *20*, 3038.
(7) Shen, S.; Torkelson, J. M. *Macromolecules* **1992**, *25*, 721.
(8) Moore, J. A. Kim, J. H. *Macromolecules* **1992**, *25*, 1427.
(9) Cesteros, L. C.; Meaurio, E.; Katime, I. *Macromolecules* **1993**, *26*, 2323.
(10) Guo, W.; Higgins, J. S. *Polymer* **1990**, *31*, 699.
(11) Kyu, T.; Saldanha, J. M. *Macromolecules* **1988**, *21*, 1021.
(12) Russell, T. P.; Hadziioannou, G.; Warburton, W. K. *Macromolecules* **1985**, *18*, 78.
(13) Lemieux, E.; Purd'homme, R. E.; Forte, R.; Jérome, R.; Teyssié, P. *Macromolecules* **1988**, *21*, 2148.
(14) Reich, S.; Cohen, Y. *J. Polym. Sci., Polym. Phys. Ed.* **1981**, *19*, 1255.
(15) Qipeng, G. *Polym. Commun.* **1990**, *31*, 217.
(16) Takahashi, M.; Kinoshita, S.; Nose, T. *J. Polym. Sci., Polym. Phys. Ed.* **1989**, *27*, 2159.
(17) Binder, K.; Stauffer, D. *Adv. Phys.* **1976**, *25*, 343.
(18) Howland, R. G.; Wong, N. C.; Knobler, C. M. *J. Chem. Phys.* **1980**, *73*, 522.
(19) Nishi, T.; Wang, T. T.; Kwei, T. K. *Macromolecules* **1975**, *8*, 227.

(20) Voigt-Martin, I. G.; Leister, K. H.; Rosenau, R.; Koningsveld, R. *J. Polym. Sci. Part B* **1986**, *24*, 723.
(21) Walsh, D. J.; Singh, V. B. *Makromol. Chem.* **1984**, *185*, 1979.
(22) Park, D. W.; Roe, R. J. *Macromolecules* **1991**, *24*, 5324.
(23) Lifshitz, I. M.; Slyozov, V. V. *J. Phys. Chem. Solids* **1961**, *19*, 35.
(24) Siggia, E. D. *Phys. Rev. A* **1979**, *20*, 595.
(25) Roe, R. J.; Zin, W. C. *Macromolecules* **1980**, *13*, 1221.
(26) Maruta, J.; Ougizawa, T.; Inoue, T. *Polymer* **1988**, *29*, 2056.
(27) Lin, J. L.; Roe, R. J. *Polymer* **1988**, *29*, 1227.
(28) Kambour, R. P.; Bendler, J. T.; Bopp, R. C. *Macromolecules* **1983**, *16*, 753.
(29) ten Brinke, G.; Karasz, F. E.; MacKnight, W. J. *Macromolecules* **1983**, *16*, 1827.
(30) Paul, D. R.; Barlow, J. W. *Polymer* **1984**, *25*, 487.